Positive parity nonstrange baryons beyond 2 GeV

P. Stassart, Fl. Stancu

Université de Liège, Institut de Physique B5, Sart Tilman,

B-4000 Liège 1, Belgium

Abstract. Previous studies of nonstrange baryons are extended to resonances of mass beyond 2 GeV, belonging to the $N = 4$ band. The framework is a semi-relativistic constituent quark model. The quark-quark interaction contains a Coulomb plus linear confinement terms and a short-range spin-spin term. It turns out that the string tension value of 1 GeV fm^{-1} fixed previously in the $N \leq 3$ bands is compatible with the $N = 4$ band. It is shown that the three-body confinement potential plays an important role in describing the inner structure of the band. The $N\pi$ decay widths are calculated in a flux-tube breaking mechanism and compared to data and other models.

PACS : 13.30Eg, 12.40Aa

1. Introduction

The purpose of the present work is to extend previous calculations [1] to high lying positive parity nonstrange resonances, those belonging to the $N = 4$ band. The number of experimentally known resonances [2] which can be identified in this band is quite restricted, but it is important to extend calculations to higher energies as this may constitute a test for the confining potential used in the model. Moreover, we calculate masses and elastic widths for a larger number than that of experimentally known resonances, and these could be considered as predictions for future analyses or a kind of guidance for new experimental investigations, for example at CEBAF.

The interest in the $N = 4$ band is not entirely new, but only a few theoretical studies are devoted to this energy range. Among them, the most extended is perhaps the work of Capstick and Isgur [3] where the calculations are performed in a large harmonic oscillabor basis. Our basis is more suited to a linear confinement and we shall compare our results to those of [3].

In our previous work, we calculated masses and strong decay widths of nonstrange resonances belonging to the $N \leq 3$ bands. These calculations were based on a semi-relativistic constituent quark model with a spin independent interaction given by a linear combination of a Coulomb plus a linear three-body confinement potential inspired by QCD and a hyperfine interaction containing a spin-spin and a tensor part. The decay widths were derived from a flux-tube breaking mechanism. The experimental spectrum and widths were generally well reproduced, with some exceptions which were recently reviewed in [4] as unsettled issues. In Sect. 2, we briefly recall the main features of the theoretical framework. In Sect. 3, we describe the procedure of finding the orthogonal set of basis states required by the symmetries of the Hamiltonian. In Sect. 4, we present our results for the spectrum and, in Sect. 5, for the strong decay widths $R \to N\pi$. Section 6 gives the conclusions.

2. The model

Our study is based on the semi-relativistic flux-tube model of Carlson, Kogut and Pandharipande and their variational wave function for the ground state [5]. The spin independent part of the Hamiltonian is

$$H_0 = \sum_i \left(p_i^2 + m^2\right)^{1/2} + V\left(\vec{r}_1, \vec{r}_2, \vec{r}_3\right) + E_0^B \tag{2.1}$$

where

$$V\left(\vec{r}_1, \vec{r}_2, \vec{r}_3\right) = \frac{1}{2} \sum_{i<j} \left(-\frac{4}{3}\frac{\alpha_S}{r_{ij}} + \sqrt{\sigma}\, r_{ij}\right) + \sqrt{\sigma}\left(\sum_i r_{i4} - \frac{1}{2}\sum_{i<j} r_{ij}\right) \tag{2.2}$$

In the three-body term, r_{i4} is the distance between the quark i and the point of equilibrium energy of a three flux-tubes meeting at $\vec{r}_4$, each tube originating from a quark source located at $\vec{r}_i$. We choose the values of the strong coupling constant α_S and the string tension $\sqrt{\sigma}$ to be

$$\frac{4}{3}\alpha_S = 0.5 , \quad \sqrt{\sigma} = 1 \text{ GeV fm}^{-1} \tag{2.3}$$

In baryon spectroscopy, the value of the string tension varies between 0.850 GeV fm^{-1} and 1 GeV fm^{-1} [6]. Here, as in our previous studies [7, 8] of the spectrum, we use the upper limit of this interval and the high lying resonances, where H_0 is the dominant part of the Hamiltonian, would be a crucial test fo this value, as discussed in Sect. 4. The constant E_0^B in (2.1) is adjusted to reproduce the nucleon mass $m_N = 940$ MeV.

To H_0, we added a short-range spin-dependent interaction of the form

$$H_{ij}^{hyp} = \frac{4\sqrt{2}\,\pi\,\alpha_S}{9\,m^2}\,\frac{1}{\left(2\,\pi\,\Lambda^2\right)^{3/2}}\,\exp\left(-\frac{r_{ij}^2}{4\,\Lambda^2}\right)\vec{S}_i\cdot\vec{S}_j \tag{2.4}$$

i.e. a regularized spin-spin interaction of the Breit-Fermi type. Here, we have neglected the tensor term because, in our previous studies, and especially that devoted to the $N=3$ band [8], we found that it brings a small contribution to interband mixings, of at most few MeV, while corrections inside a band are small as compared to those given by the spin-spin part. The remaining parameters of (2.4), i.e. the quark mass m and the finite size of the quark are set to

$$\Lambda = 0.13\ \text{fm}\ , \qquad m = 360\ \text{MeV} \tag{2.5}$$

as in the original version of the model [5] where the variational parameters of the ground state wave function $\psi_{00} = N_{00}^S\,F$ have been determined. The function F is given by the product of three two-body correlation functions $f\,(r_{ij})$ multiplied by a three-body correlation function, inspired by the form of the potential (2.2). Its form is

$$F = \left[1 - \beta\sqrt{\sigma}\left(\sum_{i=1}^{3} r_{i4} - \frac{1}{2}\sum_{i<j}^{3} r_{ij}\right)\right]\prod_{i<j} f\,(r_{ij}) \tag{2.6}$$

where

$$f(r) = \left\{ \exp - \left(\gamma_1 \, r + \gamma_2 \, r^2 \right) W(r) - \gamma_{1.5} \, r^{1.5} \left[1 - W(r) \right] \right\}$$

$$W(r) = \frac{1 + \exp\left(-r_0/a\right)}{1 + \exp\left[(r - r_0)/a\right]} \tag{2.7}$$

The variational parameters are : $\gamma_1 = 0.3965 \text{ fm}^{-1}$, $\gamma_2 = 0.637 \text{ fm}^{-2}$, $\gamma_{1.5} = 1.40 \text{ fm}^{-1.5}$, $r_0 = 0.12$ fm , $a = 0.12$ fm , $\beta = 0.25 \text{ GeV}^{-1}$

Note that the two-body correlation function f has an Airy function asymptotic behaviour

$$f(r) \underset{r \to \infty}{\longrightarrow} \exp\left(- \gamma_{1.5} \, r^{-1.5} \right) \tag{2.8}$$

appropriate for a linear confinement.

3. The excited states

To calculate the spectrum of the Hamiltonian (2.1) - (2.4), we construct a set of orthogonal wave functions for the spatial part ψ^{μ}_{L0} of the excited states, where μ is an index specifying the permutational symmetry of each three-body state. Here, $\mu = S$ stands for the symmetric, $\mu = A$ for the antisymmetric and $\mu = \rho$ or λ correspond to mixed symmetric states, which are antisymmetric and symmetric under the permutation (12), respectively. A convenient procedure to construct three-body wave functions with the correct permutation symmetries is that of Moshinski [9]. The resulting states ψ^{μ}_{L0} are polynomials of the Jacobian coordinates

$$\vec{\rho} = \frac{1}{\sqrt{2}} \left(\vec{r}_1 - \vec{r}_2 \right) , \quad \vec{\lambda} = \frac{1}{\sqrt{6}} \left(\vec{r}_1 + \vec{r}_2 - 2 \, \vec{r}_3 \right) \tag{3.1}$$

which multiply the ground state wave function. To get these polynomials for a given N, one starts from Moshinski's functions $P(n_1 \ell_1, n_2 \ell_2, LM)$ where $2n_1 + \ell_1 + 2n_2 + \ell_2 = N$, L is the total angular momentum and M is its projection. For example, for $M = 0$, one has

$$P(n_1 \ell_1, n_2 \ell_2, L0) \sim \sum \langle \ell_1 \ell_2 m - m | L0 \rangle \eta_1^{2n_1} \eta_2^{2n_2} \mathcal{Y}_{\ell_1 m}(\hat{\eta}_1) \mathcal{Y}_{\ell_2 -m}(\hat{\eta}_2) \tag{3.2}$$

where $\mathcal{Y}_{\ell m}$ are spherical harmonic functions of $\vec{\eta}_1 = -i\vec{\rho} + \vec{\lambda}$ or $\vec{\eta}_2 = i\vec{\rho} + \vec{\lambda}$. In Table 1, we indicate all possible such functions for $N = 4$, together with their permutation and SU(6) symmetries. From this table, we consider only the cases $L = 2, 3$ and 4. The others should lead to states with $J^P \leq \frac{5}{2}^+$. Keeping $L < 2$ states would bring two effects : 1) the previously calculated $N = 2$ band resonances will have new components which we expect to be negligible, as explained in the previous section and 2) the number of levels in each sector will be increased. However, there are already "missing" resonances in these sectors and one may expect that supplementary resonances are swamped in the background of the partial wave analysis, thus hard to be identified. Here, we are interested in resonances which are likely to be identified in partial wave analysis, that is resonances of higher angular momentum, namely $J^P \geq \frac{7}{2}^+$. These have no components in the $N = 2$ band, except for $J^P = \frac{7}{2}^+$. Therefore, we need only polynomials with $L \geq 2$. Among the $L=2$ polynomials, only those with $\mu = S$ are relevant for the present study. The configuration space normalized wave functions ψ^{μ}_{L0} resulting from this procedure are given in Table 2, where F is defined by (2.6) - (2.7). The states with $M \neq 0$ can be obtained from these by applying ladder operators. The two symmetric states of $L = 2$

are denoted by $\psi_{20}^{S'}$ and $\psi_{20}^{S''}$ to distinguish them from ψ_{20}^{S} belonging to the $N = 2$ band. Actually, defined as such, $\psi_{20}^{S'}$ and $\psi_{20}^{S''}$ are not orthogonal to ψ_{20}^{S} given by [7] :

$$\psi_{20}^{S} = N_{20}^{S}\left[3\left(\rho_0^2 + \lambda_0^2\right) - \left(\rho^2 + \lambda^2\right)\right] F \tag{3.3}$$

We introduce orthogonal functions as :

$$\overline{\Psi}_{20}^{S'} = \overline{N}_{20}^{S'}\left(\psi_{20}^{S} + c' \, \psi_{20}^{S'}\right) \tag{3.4}$$

$$\overline{\Psi}_{20}^{S''} = \overline{N}_{20}^{S''}\left(\psi_{20}^{S} + c''_1 \, \overline{\Psi}_{20}^{S'} + c''_2 \, \overline{\Psi}_{20}^{S''}\right) \tag{3.5}$$

where the coefficients c' and c'' are determined by orthogonalization. The calculation of these coefficients as well as of the norms has been performed in two ways. One is by reducing 6-dimensional integrals in the $\vec{\rho}$ and $\vec{\lambda}$ variables to 3-dimensional integrals as in [7], the other is by the Monte-Carlo method. Their values are given in Table 3. An advantage of using the functions of Table 2 over a harmonic oscillator expansion, as in [3], is that there is no problem of convergence and the compact form of those functions is practical in the calculation of the widths, as performed in Sect. 5.

4. The spectrum

Here, we present results for the spectrum of the $N = 4$ band resonances based on the Hamiltonian model of Sect. 2. First, we discuss the pattern of levels resulting from the spin-independent part H_0 of the Hamiltonian, inasmuch as we wish to test the confinement. The spin-dependent part will bring corrections of only a few percent to the expectation values of H_0 and its role is to introduce mixings between configurations. These mixings are most important in the calculation of the widths, as we shall see in the next section. In Table 4, we exhibit the expectation values of H_0 for the selected SU(6) multiplets relevant for this study (see previous section). The required wave functions are those of Table 2 and (3.4) and (3.5). Detailed contributions to $\langle H_0 \rangle$ are also indicated : the kinetic energy, the Coulomb part and the two- and three-body parts, respectively.

For completeness, we also added the value associated to $(56, 0^+)$. The constant E_0^B was determined to be - 1.393 GeV in order to fit the $(56, 0^+)$ expectation value to 1.086 GeV , which is the average mass of nucleon and the $\Delta(1232)$ resonance.

From Table 4 and Fig. 1, one can see that the Coulomb and two-body confinement distinguish little - by at most 40 MeV - between various multiplets inside the $N = 4$, while the kinetic and the three-body parts distinguish much more, up to 90 MeV. Addition of all contributions makes a spread of over 200 MeV in the spectrum of H_0 , the lowest state $(56, 4^+)$ being located at 2367 MeV and the highest $(70, 3^+)$ at 2580 MeV . The fact that the kinetic energy and the three-body confinement part distinguish between states inside a band, more than the Coulomb and the two-body confinement, shows that they have a crucial role in the level ordering inside a band. By contrast, the contribution of the three-body confinement to the gap between bands is minor, the dominant contributions being the kinetic and the two-body confinement parts. Thus, although the three-body contribution to the entire expectation value of H_0 is of the order of 10-15 %, it should however be regarded as an important ingredient of the Hamiltonian model (2.1)-(2.2).

By including the spin and flavour degrees of freedom, one can notice that the $(56, 4^+)$ gives rise, in particular, to a pure nucleon $\frac{11}{2}^+$ state. As it will be seen below, the hyperfine interaction (2.4) shifts the value of $\langle H_0 \rangle$ associated to $(56, 4^+)$ by few tens of MeV, in the right direction. One can then conclude that the basic features of H_0 and the value (2.3) chosen for the string tension bear no hint of being inappropriate for the $N = 4$ band. By incorporating spin and flavour degrees of freedom to the configuration space states described in Sect. 3, we have obtained the basis states in which the Hamiltonian (2.1)-(2.4), with the parameters (2.5), has been diagonalized. The results are presented in Table 5. The space parts of the matrix elements of H_0 are six-dimensional integrals calculated with a Monte-Carlo method, with a precision of under 1% for the ground state and 2-3% for the excited states where the increase in the statistical error stems from the kinetic energy part, which must be handled with care [10]. In the same table, some results of [3] are also presented for comparison, and the few known experimental masses are also indicated. Note that the sector $\frac{7}{2}^+$ is the only one containing an $N = 2$ band multiplet, namely the $(56, 2^+)$. From Table 5, one can see that the agreement of the calculated spectrum with the experimental masses is quite satisfactory at this level, where coupling to baryon-meson channels, which is generally expected to produce few tens of MeV shifts [11], has been ignored. An important aspect is that there is no striking disagreement as it exists in the $N = 3$ sector with the $D_{35}(1930)$ resonance [8].

5. $N\pi$ decay widths

The calculation of the decay widths have been performed within a flux-tube-breaking mechanism, as described in [12]. Here, we have used the limit of an infinite extension flux-tube because it provides a very good approximation to a finite-extension, QCD-inspired, flux-tube breaking, and is much simpler [12, 13]. In this limit, commonly called the $^3P_0$ quark creation model, the decay amplitude of a resonance B^* into a baryon B and a meson M reads :

$$<BM|T|B^*>^{J_{B^*}}_{m_B m_N} = \sum_m <11\ m\ -m|00> <\phi_B^{m_B}\ \phi_M^{m_M}|\phi_{B^*}\ \phi_{vac}^{-m}> I_m\,(B^*;B,M) \tag{5.1}$$

where J_{B^*} is the total angular momentum of B^* and m_B and m_N are the spin projections in the final state. The ϕ 's are the spin-flavour part of the wave functions, including the vacuum state ϕ_{vac}^{-m} of $J^{PC} = 0^{++}$ from which a $q\bar{q}$ pair is created. The factor $I_m\,(B^*;B,M)$ is the overlap integral containing the configuration space wave functions ψ

$$I_m\,(B^*;B,M) = -\left(\frac{3}{4\pi}\right)^{1/2} \frac{2^3}{(2\pi)^{3/2}}\, \delta\left(\vec{k}_M + \vec{k}_B\right)\gamma_0 \int d^3\rho\, d^3\lambda\, d^3x$$

$$\times\ \psi_{B^*}\left[\vec{\rho}, \vec{\lambda} + \left(\frac{8}{3}\right)^{1/2}\vec{x}\right] \psi_B\left(\vec{\rho},\vec{\lambda}\right) \exp\left\{i\vec{k}_M\cdot\left[\left(\frac{2}{3}\right)^{1/2}\vec{\lambda} + \vec{x}\right]\right\}$$

$$\times\ \vec{\varepsilon}_m\cdot\left(\vec{k}_M + i\vec{\nabla}_x\right)\psi_M\,(2\,\vec{x}) \tag{5.2}$$

Here, $\vec{k}_M$ and $\vec{k}_B$ are the momenta of the final state, in the resonance frame, $\vec{\varepsilon}_m$ is a spherical unit vector. The non-local character of a finite size emitted meson $\psi_M\,(\vec{x}) \neq \delta\,(\vec{x})$ is explicitly indicated by the dependence of ψ_{B^*} on $\vec{x}$. The quantity γ_0 is the breaking amplitude parameter, which is a constant, in the infinite flux-tube limit. This parameter has been fit to reproduce the $\Delta\,(1232) \rightarrow N\pi$ decay width, so that the present calculations are parameter free.

The transition amplitudes (5.2) are converted into helicity amplitudes $M^{J_{B*}}_{\ell s}$ by using the Jacob-Wick formula, where ℓ and s are the relative orbital momentum and the total spin of the outgoing particles. Then, a partial decay width in the resonance rest frame is defined by

$$\Gamma_{\ell s} = \frac{1}{\pi} \frac{\left|M^{J_{B*}}_{\ell s}\right|^2}{2\, J_{B*} + 1} \frac{k\, E_M\, E_B}{M_{B*}} < I_B\, I_M\, I_{3\,B} I_{3\,M} \mid I_{B*}\, I_{3\,B*} >^{-2} \tag{5.3}$$

where $k = k_M = k_B$, M_{B*} is the resonance mass and the E 's are the relativistic energies of the outgoing particles. Since the outgoing baryon is the ground state nucleon, i.e. $J_B = \frac{1}{2}$, there is only one transition wave ℓs, hence $\Gamma_{N\pi} = \Gamma_{\ell s}$ [10] for each resonance. In Table 6, we present the decay amplitudes defined as $\Gamma^{1/2}_{N\pi}$, derived from the formula (5.3). We compare our results to those of Capstick and Roberts [14] and with the experiment, when available [2, 15]. In [14], the same decay mechanism, the pair creation model has been used and we can notice a large similarity between our results and those of [14] although their mass spectrum results from a somewhat different Hamiltonian [3]. An important difference appears for the H_{19} (2220) resonance where we are closer to the experimental value, both for the mass and the decay width. In fact, the theoretical mass of 2345 MeV used in [14] increases the phase space volume which means that the $N\pi$ width of that state would differ even more when using the experimental mass as a calculation input. Concerning the three 4-star resonances of Table 6, the largest discrepancy with the data appears for the $H_{3,11}$ (2420) resonance, which is difficult to understand. However, the important outcome is that for resonances where data are missing, the decay amplitudes are small, with one exception, the 5-th F_{37} resonance, where $\Gamma^{1/2}_{N\pi} = 12.9\ \mathrm{MeV}^{1/2}$, which may explain why these resonances would not be "seen" in partial wave analysis.

6. Conclusions

We have calculated the spectrum and $N\pi$ decay widths of nonstrange baryon resonances belonging to the $N = 4$ band. The calculated masses of the states under study are in the range 2360 MeV - 2550 MeV . This is a range where the kinetic energy and the confinement potential are the dominant terms in the spin-independent part of the potential. We found out that the three-body part of the confinement plays an important role in determining the level ordering inside the band. The calculated masses are in satisfactory agreement with the few available experimental data. The other values can be considered as predictions.

We calculated $N\pi$ decay widths and compared our results to those of Capstick and Roberts. We found that they are very similar. Our Hamiltonian and strong decay mechanism is a QCD-inspired flux-tube model, as is that of Capstick and Roberts. However, the parametrization is different and the practical calculations are different. We work with compact expressions for the space-part of the wave functions, with the asymptotic behaviour required by a linear confinement potential, while they use a harmonic-oscillator expansion. In both cases, the widths are smaller than the mean values of the experimentally observed ones. For the four-star resonances, our calculated amplitudes range from 65 % to 98 % of the lower bound of the experimental value. The present calculations perhaps give a hint of why so few high-lying resonances have been seen in the partial wave analysis. Indeed, our calculations indicate that the "unseen" resonances have a very small $N\pi$ width, except for one. In the spirit of the CEBAF projects, it would be interesting to see if they couple to other channels. Thus, they should be searched for in inelastic channels.

References

1. Stassart, P., Stancu, Fl. : Z. Phys. A **351**, 77 (1995), and references therein
2. Particle Data Group : Phys. Rev. D **54** (1996)
3. Capstick, S., Isgur, N. : Phys. Rev. D **34**, 2809 (1986)
4. Stassart, P., Stancu, Fl. : In : Quark Confinement and the Hadron Spectrum II, Brambilla, N., Prosperi , G.M. (eds.). Singapore : World Scientific 1997
5. Carlson, J., Kogut, J., Pandharipande, V.R. : Phys. Rev. D **27**, 233 (1983)
6. Blask, W., Huber, H.G., Metsch, B.C. : Z. Phys. A **326**, 413 (1987) ; Zeng, J., Van Orden, J.W., Roberts, W. : Phys. Rev. D **52**, 5229 (1995) ; Barnes, T., Close, F.E., Swanson, E.S. : Phys. Rev. D **52**, 5242 (1995)
7. Sartor, R., Stancu, Fl. : Phys. Rev. D **33**, 727 (1986)
8. Stancu, Fl., Stassart, P. : Phys. Lett. B **269**, 243 (1991)
9. Moshinski, M. : The Harmonic Oscillator in Modern Physics : From Atoms to Quarks. New York : Gordon and Breach 1969
10. Stassart, P. : Ph.D. Thesis, University of Liège 1991
11. Silvestre-Brac, B., Gignoux, C. : Phys. Rev. D **43**, 3699 (1991)
12. Stancu, Fl., Stassart, P. : Phys. Rev. D **39**, 343 (1989)
13. Kokoski, R., Isgur, N. : Phys. Rev. D **35**, 907 (1987)
14. Capstick, S., Roberts, W. : Phys. Rev. D **47**, 1994 (1993) ; D **49**, 4570 (1994)
15. Cutkoski, R.E., Forsyth, C.P., Hendrik, R.E., Kelly, R.L. : Phys. Rev. D **20**, 2839 (1979).

Figure caption

Figure 1 : The H_0 parts expectation value (MeV) for SU(6) multiplets in the $N = 4$ band, counted from the lowest $N = 4$ value for each part (kinetic, Coulomb, 2-body confinement, 3-body confinement).

Table Caption

Table 1 : All possible polynomials $P(n_1 \ell_1, n_2 \ell_2, LM)$ of degree $N = 4$ and permutation symmetry μ corresponding to states of L units of angular excitations and $n_1 + n_2$ units of radial excitations. M is the projection of the angular momentum. The sign + corresponds to λ or S and - to ρ or A symmetry, respectively. The last column gives the corresponding SU(6) notation.

Table 2 : $N = 4$ configuration space wavefunctions ψ^{μ}_{L0} in terms of Jacobi coordinates $(\vec{\rho}, \vec{\lambda})$; F is defined by (2.6) ; N^{μ}_{L0} stands for normalization factor ; $\rho_{\pm} = \rho_x \pm i \rho_y$, etc.

Table 3 : Numerical values of some constants appearing in the functions of Table 2 and Equations (3.3)-(3.5). The unspecified ones can be calculated from the relations $\left(N^{\lambda}_{40}\right)^{-1} = 4\left(N^{\rho}_{40}\right)^{-1}$, $\left(N^{\lambda'}_{40}\right)^{-1} = 2\left(N^{\rho'}_{40}\right)^{-1}$, $\left(N^{\lambda}_{30}\right)^{-1} = 0.5\left(N^{\rho}_{30}\right)^{-1}$ obtained analytically.

Table 4 : Expectation values (MeV) for various SU(6) symmetry states. 1st column : multiplet ; 2nd : kinetic energy plus E^B_0 ; 3rd : Coulomb ; 4th : confinement (2-body) ; 5th : confinement (3-body) ; 6th : expectation value of H_0 of (2.1). Unless specified, symmetries are for $N = 4$ states. The last two rows are expectation values for $\overline{\psi}^{S'}_{20}$ eq. (3.4) and $\overline{\psi}^{S''}_{20}$ eq. (3.5).

Table 5 : High-lying nonstrange baryons of positive parity. Column 1 : the state. Column 2 : mass spectrum (MeV) of the present work. Column 3 : mixing angles, present work. Column 4 : spectrum of [3]. Column 5 : experiment [2].

Table 6 : Square root of the decay width $\Gamma_{N\pi}^{1/2}$ (MeV$^{1/2}$) . Experimental values for 4-star resonances are from PDG [2], those of 1- or 2-star resonances are from [15].

Table 1

L	Polynomial	μ	SU(6) multiplet
4	P(04, 00, 4M) ± P(00, 04, 4M)	λ, ρ	$(70, 4^+)$
	P(03, 01, 4M) ± P(01, 03, 4M)	λ, ρ	$(70', 4^+)$
	P(02, 02, 4M)	S	$(56, 4^+)$
3	P(03, 01, 3M) ± P(01, 03, 3M)	λ, ρ	$(70, 3^+)$
	P(02, 02, 3M)	A	$(20, 3^+)$
2	P(03, 01, 2M) ± P(01, 03, 2M)	λ, ρ	$(70', 2^+)$
	P(02, 02, 2M)	S	$(56', 2^+)$
	P(11, 01, 2M) ± P(01, 11, 2M)	λ, ρ	$(70'', 2^+)$
	P(12, 00, 2M) ± P(00, 12, 2M)	λ, ρ	$(70''', 2^+)$
	P(10, 02, 2M) ± P(02, 10, 2M)	S, A	$(56'', 2^+)$, $(20, 2^+)$
1	P(11, 01, 1M) ± P(01, 11, 1M)	λ, ρ	$(70, 1^+)$
	P(02, 02, 1M)	A	$(20', 1^+)$
0	P(11, 01, 00) ± P(01, 11, 00)	λ, ρ	$(70', 0^+)$
	P(10, 10, 00)	S	$(56'', 0^+)$
	P(20, 00, 00) ± P(00, 20, 00)	λ, ρ	$(70'', 0^+)$
	P(02, 02, 00)	S	$(56''', 0^+)$

Table 2

$$\psi_{40}^{S} = N_{40}^{S}\left[3\left(\rho^4+\lambda^4\right)+35\left(\rho_0^2+\lambda_0^2\right)^2-30\left(\rho^2\rho_0^2+\lambda^2\lambda_0^2\right)\right.$$

$$\left.+2\left(\rho^2\lambda^2-5\rho^2\lambda_0^2-5\rho_0^2\lambda^2\right)+4\vec{\rho}\cdot\vec{\lambda}\left(\vec{\rho}\cdot\vec{\lambda}-10\rho_0\lambda_0\right)\right]F$$

$$\psi_{40}^{\rho} = N_{40}^{\rho}\left[35\rho_0\lambda_0\left(\rho_0^2-\lambda_0^2\right)-15\rho_0\lambda_0\left(\rho^2-\lambda^2\right)-15\vec{\rho}\cdot\vec{\lambda}\left(\rho_0^2-\lambda_0^2\right)+3\left(\rho^2-\lambda^2\right)\vec{\rho}\cdot\vec{\lambda}\right]F$$

$$\psi_{40}^{\lambda} = N_{40}^{\lambda}\left\{-35\left(\rho_0^4-6\rho_0^2\lambda_0^2+\lambda_0^4\right)+30\left[\left(\rho^2-\lambda^2\right)\left(\rho_0^2-\lambda_0^2\right)-4\vec{\rho}\cdot\vec{\lambda}\rho_0\lambda_0\right]\right.$$

$$\left.-3\left(\rho^2-\lambda^2\right)^2+12\left(\vec{\rho}\cdot\vec{\lambda}\right)^2\right\}F$$

$$\psi_{40}^{\rho'} = N_{40}^{\rho'}\left[35\rho_0^3\lambda_0+35\rho_0\lambda_0^3-15\left(\rho_0^2+\lambda_0^2\right)\vec{\rho}\cdot\vec{\lambda}-15\left(\rho^2+\lambda^2\right)\rho_0\lambda_0+3\left(\rho^2+\lambda^2\right)\vec{\rho}\cdot\vec{\lambda}\right]F$$

$$\psi_{40}^{\lambda'} = N_{40}^{\lambda'}\left[35\left(\rho_0^4-\lambda_0^4\right)-30\left(\rho^2\rho_0^2-\lambda^2\lambda_0^2\right)+3\left(\rho^4-\lambda^4\right)\right]F$$

$$\psi_{30}^{A} = N_{30}^{A}\left(\rho_+\lambda_--\rho_-\lambda_+\right)\left[5\left(\rho_0^2+\lambda_0^2\right)-\left(\rho^2+\lambda^2\right)\right]F$$

$$\psi_{30}^{\rho} = N_{30}^{\rho}\left(\rho_+\lambda_--\rho_-\lambda_+\right)\left[5\left(\rho_0^2-\lambda_0^2\right)-\left(\rho^2-\lambda^2\right)\right]F$$

$$\psi_{30}^{\lambda} = N_{30}^{\lambda}\left(\rho_+\lambda_--\rho_-\lambda_+\right)\left(\vec{\rho}\cdot\vec{\lambda}-5\rho_0\lambda_0\right)F$$

$$\psi_{20}^{S'} = N_{20}^{S'}\left[\rho^4+\lambda^4-3\left(\rho^2\rho_0^2+\lambda^2\lambda_0^2\right)+10\rho^2\lambda^2-15\left(\rho_0^2\lambda^2+\rho^2\lambda_0^2\right)-8\vec{\rho}\cdot\vec{\lambda}\left(\vec{\rho}\cdot\vec{\lambda}-3\rho_0\lambda_0\right)\right]F$$

$$\psi_{20}^{S''} = N_{20}^{S''}\left[3\left(\rho^2-\lambda^2\right)\left(\rho_0^2-\lambda_0^2\right)+12\rho_0\lambda_0\vec{\rho}\cdot\vec{\lambda}-\left(\rho^2-\lambda^2\right)^2-4\left(\vec{\rho}\cdot\vec{\lambda}\right)^2\right]F$$

Table 3

$\left(N_{20}^{S}\right)^{-1}$	0.05921
$\left(N_{40}^{S}\right)^{-1}$	0.13507
$\left(N_{40}^{\rho}\right)^{-1}$	0.05290
$\left(N_{40}^{\rho'}\right)^{-1}$	0.05725
$\left(N_{30}^{A}\right)^{-1}$	0.02271
$\left(N_{30}^{\rho}\right)^{-1}$	0.02214
$\left(N_{20}^{S'}\right)^{-1}$	0.07519
$\left(N_{20}^{S''}\right)^{-1}$	0.04636
c'	1.21271
c''_1	- 0.14655
c''_2	- 1.19486
$\left(\overline{N}_{20}^{S'}\right)^{-1}$	0.68606
$\left(\overline{N}_{20}^{S''}\right)^{-1}$	0.63735

Table 4

Multiplet	K.E. + E_0^B	Coulomb	2-body conf.	3-body conf.	$\langle H_0 \rangle$
$(56, 0^+)$ (N = 0)	496	- 345	854	80	1086
$(56, 2^+)$ (N = 2)	757	-242	1216	94	1825
$(56, 4^+)$	943	- 199	1524	98	2367
$(70, 4^+)$	983	- 171	1548	164	2524
$(70', 4^+)$	922	- 191	1531	115	2377
$(20, 3^+)$	994	- 167	1550	169	2547
$(70, 3^+)$	1002	- 162	1555	185	2580
$(\overline{56}', 2^+)$	937	- 192	1530	169	2444
$(\overline{56}'', 2^+)$	963	- 195	1518	128	2415

Table 5

(1)	(2)	(3)							(4)	(5)
$^4\Delta\,(56,2^+)\,\frac{7}{2}^+$	1852	0.999	-0.045	-0.010	0	0	0	0	1940	1950
$^4\Delta\,(\overline{56}',2^+)\,\frac{7}{2}^+$	2366	0	0	0	0	-0.167	0.986	0		
$^4\Delta\,(\overline{56}'',2^+)\,\frac{7}{2}^+$	2381	0	0	0	1	0	0	0	2370	2390
$^4\Delta\,(56,4^+)\,\frac{7}{2}^+$	2415	-0.009	-0.412	0.911	0	0	0	0		
$^2\Delta\,(70,4^+)\,\frac{7}{2}^+$	2463	-0.045	-0.910	-0.412	0	0	0	0		
$^2\Delta\,(70',4^+)\,\frac{7}{2}^+$	2505	0	0	0	0	-0.986	-0.167	0		
$^2\Delta\,(70,3^+)\,\frac{7}{2}^+$	2550	0	0	0	0	0	0	1		
$^2N\,(56,4^+)\,\frac{9}{2}^+$	2268	0.762	0.115	0.638	0	0	0		2345	2220
$^2N\,(70,4^+)\,\frac{9}{2}^+$	2377	-0.631	-0.092	0.770	0	0	0			
$^2N\,(70',4^+)\,\frac{9}{2}^+$	2384	0	0	0	-0.063	0.998	0			
$^4N\,(70,4^+)\,\frac{9}{2}^+$	2498	0.147	-0.989	0.003	0	0	0			
$^4N\,(70',4^+)\,\frac{9}{2}^+$	2518	0	0	0	-0.998	-0.063	0			
$^4N\,(70,3^+)\,\frac{9}{2}^+$	2567	0	0	0	0	0	1			

Table 5

$^4\Delta\,(56, 4^+)\,\frac{9}{2}^+$	2366	0	-0.167	0.985	2420	2300
$^2\Delta\,(70, 4^+)\,\frac{9}{2}^+$	2381	1	0	0		
$^2\Delta\,(70', 4^+)\,\frac{9}{2}^+$	2505	0	-0.986	-0.167		
$^4N\,(70, 4^+)\,\frac{11}{2}^+$	2384		-0.063	0.998		
$^4N\,(70', 4^+)\,\frac{11}{2}^+$	2518		0.998	0.063		
$^4\Delta\,(56, 4^+)\,\frac{11}{2}^+$	2381		1		2450	2420

Table 6

Resonance	Main component	This work	Ref. [14]	Experiment	
F_{37} (1950)	$^4\Delta\,(56, 2^+)\,\frac{7}{2}^+$	6.4	7.1 ± 0.1	$10.6\,^{+1.2}_{-0.5}$	****
F_{37}	$^2\Delta\,(70', 4^+)\,\frac{7}{2}^+$	0.7			
F_{37} (2390)	$^4\Delta\,(56, 4^+)\,\frac{7}{2}^+$	2.4	$1.5\,^{+0.6}_{-0.9}$	$4.9\,^{+2.0}_{-2.1}$	*
F_{37}	$^4\Delta\,(\overline{56}'', 2^+)\,\frac{7}{2}^+$	1.5			
F_{37}	$^4\Delta\,(\overline{56}', 2^+)\,\frac{7}{2}^+$	12.9			
F_{37}	$^2\Delta\,(70, 4^+)\,\frac{7}{2}^+$	0.1			
F_{37}	$^2\Delta\,(70, 3^+)\,\frac{7}{2}^+$	0.4			
H_{19} (2220)	$^2N\,(56, 4^+)\,\frac{9}{2}^+$	5.6	$3.6\,^{+0.9}_{-0.8}$	$7.7\,^{+2.8}_{-2.0}$	****
H_{19}	$^2N\,(70', 4^+)\,\frac{9}{2}^+$	0.2			
H_{19}	$^4N\,(70', 4^+)\,\frac{9}{2}^+$	0.9			
H_{19}	$^2N\,(70, 4^+)\,\frac{9}{2}^+$	2.2			
H_{19}	$^4N\,(70, 4^+)\,\frac{9}{2}^+$	0.6			
H_{19}	$^4N\,(70, 3^+)\,\frac{9}{2}^+$	0.3			
H_{39} (2300)	$^2\Delta\,(70', 4^+)\,\frac{9}{2}^+$	1.7	$1.2\,^{+0.5}_{-0.4}$	$5.0\,^{+1.8}_{-1.7}$	**
H_{39}	$^4\Delta\,(56, 4^+)\,\frac{9}{2}^+$	1.5			
H_{39}	$^2\Delta\,(70, 4^+)\,\frac{9}{2}^+$	1.0			
$H_{1,11}$	$^4N\,(70', 4^+)\,\frac{11}{2}^+$	1.8			
$H_{1,11}$	$^4N\,(70, 4^+)\,\frac{11}{2}^+$	1.4			
$H_{3,11}$ (2420)	$^4\Delta\,(56, 4^+)\,\frac{11}{2}^+$	2.4	2.9 ± 0.7	$6.3\,^{+2.4}_{-2.4}$	****

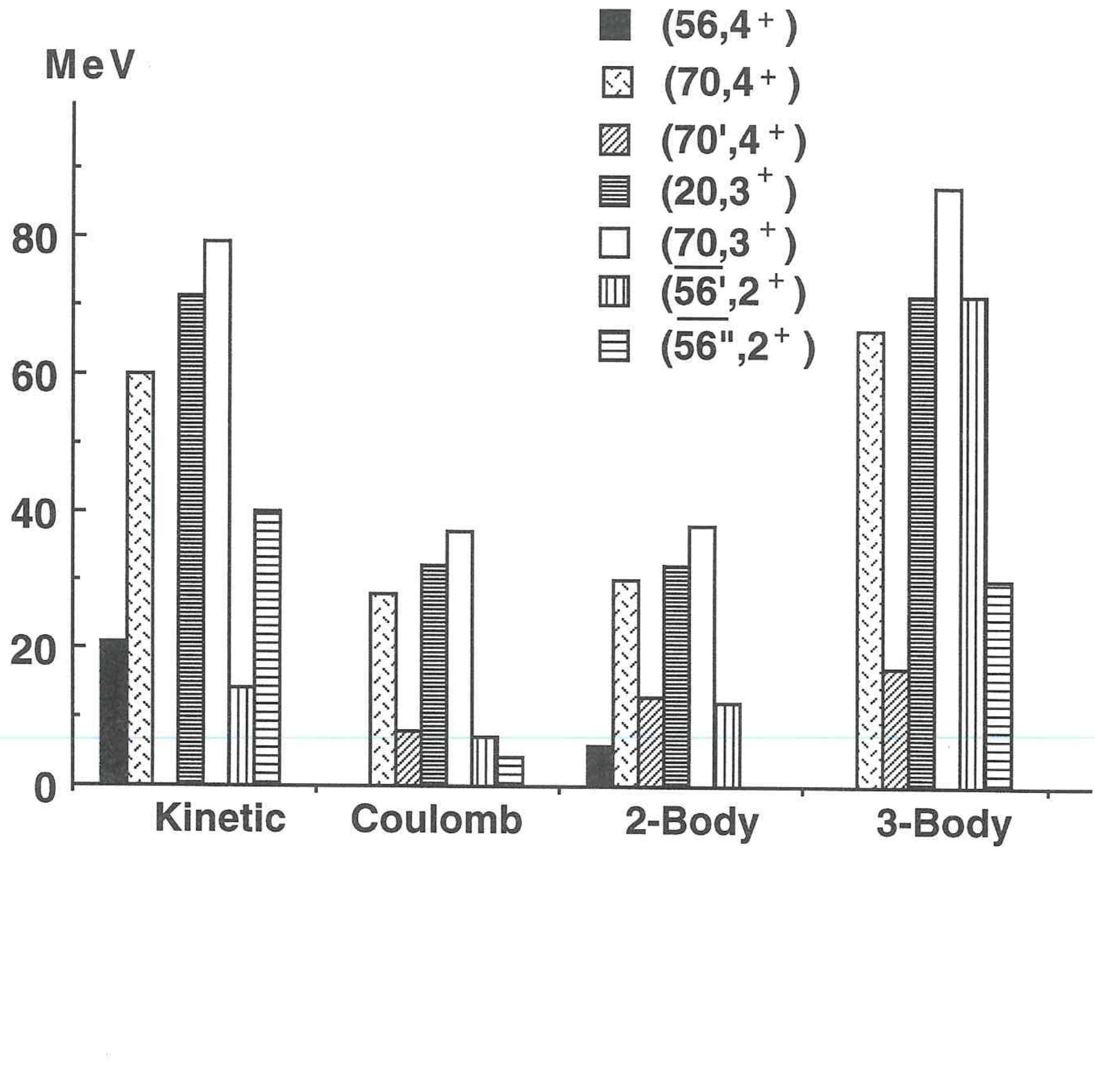
MeV
80
60
40
20
0
(56,4$^+$)
(70,4$^+$)
(70',4$^+$)
(20,3$^+$)
(70,3$^+$)
(56',2$^+$)
(56'',2$^+$)
Kinetic
Coulomb
2-Body
3-Body